Spatio-temporal landscape modelling for natural hazard vulnerability analysis in select watersheds of Central Western Ghats

T. V. Ramachandra, *Senior Member, IEEE*, Anindita Dasgupta,Uttam Kumar, *Student Member, IEEE,* Bharath H Aithal, *Student Member, IEEE,* P. G. Diwakar and N. V. Joshi

***Abstract*—Natural hazards such as landslides are triggered by numerous factors such as ground movements, rock falls, slope failure, debris flows, slope instability, etc. Changes in slope stability happen due to human intervention, anthropogenic activities, change in soil structure, loss or absence of vegetation (changes in land cover), etc. Loss of vegetation happens when the forest is fragmented due to anthropogenic activities. Hence land cover mapping with forest fragmentation can provide vital information for visualising the regions that require immediate attention from slope stability aspects. The main objective of this paper is to understand the rate of change in forest landscape from 1973 to 2004 through multi-sensor remote sensing data analysis. The forest fragmentation index presented here is based on temporal land use information and forest fragmentation model, in which the forest pixels are classified as patch, transitional, edge, perforated, and interior, that give a measure of forest continuity. The analysis carried out for five prominent watersheds of Uttara Kannada district– Aganashini, Bedthi, Kali, Sharavathi and Venkatpura revealed that interior forest is continuously decreasing while patch, transitional, edge and perforated forest show increasing trend. The effect of forest fragmentation on landslide occurrence was visualised by overlaying the landslide occurrence points on classified image and forest fragmentation map. The increasing patch and transitional forest on hill slopes are the areas prone to landslides, evident from the field verification, indicating that deforestation is a major triggering factor for landslides. This emphasises the need for immediate conservation measures for sustainable management of the landscape. Quantifying and describing land use - land cover change and fragmentation is crucial for assessing the effect of land management policies and environmental protection decisions.**

***Index Terms*—Forest fragmentation, landslide, SVM, MLC**

T. V. Ramachandra is with the Centre for Ecological Sciences, Centre for Sustainable Technologies and Centre for *Infrastructure*, Sustainable Transport and Urban Planning, Indian Institute of Science, Bangalore, India. (Corresponding author phone: 91-80-23600985/22932506/22933099; fax: 91-80-23601428/23600085; e-mail: cestvr@ces.iisc.ernet. in, energy@ces.iisc.ernet.in)

Anindita Dasgupta is with the Centre for Ecological Sciences, Indian Institute of Science, Bangalore, India. (e-mail:anindita_dasgupta@ces.iisc. ernet.in)

Uttam Kumar is with the Department of Management Studies and Centre for Sustainable Technologies, Indian Institute of Science, Bangalore, India. (e-mail: uttam@ces.iisc.ernet.in)

Bharath H Aithal is with the Centre for Sustainable Technologies, Indian Institute of Science, Bangalore, India. (e mail:bharath@ces.iisc.ernet.in)

P. G. Diwakar is with the RRSSC, Indian Space Research Organization, Department of Space, Government of India, Banashanakari, Bangalore 70. (e-mail: diwakar@isro.gov.in)

N. V. Joshi is with the Centre for Ecological Sciences, Indian Institute of Science, Bangalore, India (e-mail: nvjoshi@ces.iiec.ernet.in)

ISTC/BES/TVR/205 (2007-2010)

I. INTRODUCTION

Natural hazards such as landslides involving small to large ground movements are mainly triggered due to unstable slopes with scanty green cover. Unstable sloped are induced due to the removal of vegetation cover, rock falls, deep failure of slopes, shallow debris flows, ground water pressure, erosion, soil nutrients, soil structure, etc. The actual landslide often requires a trigger before being released and in most cases, a change in land cover (LC) due to the loss of vegetation is a primary factor that builds up specific sub-surface conditions for landslide to occur. The loss in forest cover due to LC change has increased rapidly in recent times due to increasing mankind needs. Forest cover is reduced to almost half of the ecologically desired amount [1] and about 72 percent of India's forests have lost their viability for regeneration, with forest grazing being one of the most important causes [2]. Forest fragmentation apart from affecting the biodiversity and ecology of the region has a significant influence in the movement of soil (silt) and debris in undulating terrains with high intensity rainfall. Forest fragmentation analysis spatially aids in visualising the regions that require immediate attention to minimise natural calamities such as landslides. Spatial fragmentation map depicts the type and extent of fragmentation derived from land use (LU) data which are obtained from multi-source, multi-sensor, multi-temporal, multi-frequency or multi-polarization remote sensing (RS) data. The objectives of this paper are

i.) Classification of multi-temporal RS data using Maximum Likelihood classifier to obtain LU map.
ii.) Multi-temporal forest fragmentation analysis for five watersheds in Uttara Kannada to characterise the type and extent of fragmentation or loss of vegetation cover.
iii.) Visualising the consequences of fragmentation for landslide susceptibility.

II. METHODS

A. Maximum Likelihood classifier (MLC) – Supervised classification of the image was performed using MLC. MLC has become popular and widespread in RS because of its robustness [3–6]. It quantitatively evaluates both the variance and covariance of the category spectral response pattern [7] assuming the distribution of data points to be Gaussian [8] which is described by the mean vector and the covariance matrix. The statistical probability of a given pixel value being a member of a particular class is computed and the pixel is assigned to the most likely class (highest probability value). If the training data pertaining to different classes contain *n* samples and the samples in each class are

i.i.d. (independent and identically distributed) random variables and further if we assume that the spectral classes for an image is represented by ω_n, n=1,…, N, where N is the total number of classes, then probability density $p(\omega_n|\mathbf{x})$ gives the likelihood that the pixel **x** belongs to class ω_n where **x** is a column vector of the observed digital number of the pixels. It describes the pixel as a point in multispectral space (M-dimensional space, where M is the number of spectral bands). The maximum likelihood (ML) parameters are estimated from representative i.i.d. samples. Classification is performed according to

$$x \in \omega_n \text{ if } p(\omega_n \mid x) > p(\omega_j \mid x) \ \forall \ j \neq n \qquad (1)$$

i.e., the pixel x belongs to class ω_n if $p(\omega_n|\mathbf{x})$ is largest. The ML decision rule is based on a normalised estimate of the probability density function (p.d.f.) of each class. The discriminant function, $g_{ln}(\mathbf{x})$ for ω_n in MLC is expressed as

$$g_{ln}(\mathbf{x}) = p(x|\omega_n)p(\omega_n) \qquad (2)$$

where $p(\omega_n)$ is the prior probability of ω_n, $p(\mathbf{x}|\omega_n)$ is the p.d.f. for pixel vector **x** conditioned on ω_n [6]. Pixel vector **x** is assigned to the class for which $g_{ln}(\mathbf{x})$ is greatest. In an operational context, the logarithm form of (2) is used, and after the constants are eliminated, the discriminant function for ω_n is stated as

$$G_{ln}(\mathbf{x}) = (\mathbf{x} - \mu_n)^T \sum_n^{-1} (\mathbf{x} - \mu_n) + \ln |\sum_n| - 2 \ln P(\omega_n) \qquad (3)$$

where $\sum_n$ is the variance-covariance matrix of ω_n, μ_n is the mean vector of ω_n. A pixel is assigned to the class with the lowest $G_{ln}(\mathbf{x})$ [6, 9-10]. For each LU class (agricultural land, human settlement / residential / commercial areas, roads, forest, plantation, waste land / open land and water bodies) training samples were collected representing approximately 10% of the study area. With these 10% known pixel labels from training data, the aim was to assign labels to all the remaining pixels in the image.

B. Forest fragmentation: Forest fragmentation is the process whereby a large, continuous area of forest is both reduced in area and divided into two or more fragments. The decline in the size of the forest and the increasing isolation between the two remnant patches of the forest has been the major cause of declining biodiversity [11-15]. The primary concern is direct loss of forest area, and all disturbed forests are subject to "edge effects" of one kind or another. Forest fragmentation is of additional concern, insofar as the edge effect is mitigated by the residual spatial pattern [16-19].

LU map indicate only the location and type of forest, and further analysis is needed to quantify the forest fragmentation. Total extent of forest and its occurrence as adjacent pixels, fixed-area windows surrounding each forest pixel is used for calculating type of fragmentation. The result is stored at the location of the centre pixel. Thus, a pixel value in the derived map refers to between-pixel fragmentation around the corresponding forest location. As an example [20], if *Pf* is the proportion of pixels in the window that are forested and *Pff* is the proportion of all adjacent (cardinal directions only) pixel pairs that include at least one forest pixel, for which both pixels are forested. Pff estimates the conditional probability that, given a pixel of forest, its neighbour is also forest. The six fragmentation model that identifies six fragmentation categories are: (1) interior, for which Pf = 1.0; (2), patch, Pf < 0.4; (3) transtitional, 0.4 < Pf < 0.6; (4) edge, Pf > 0.6 and Pf-Pff > 0; (5) perforated, Pf > 0.6 and Pf-Pff < 0, and (6) undetermined, Pf > 0.6 and Pf = Pff. When Pff is larger than Pf, the implication is that forest is clumped; the probability that an immediate neighbour is also forest is greater than the average probability of forest within the window. Conversely, when Pff is smaller than Pf, the implication is that whatever is non-forest is clumped. The difference (Pf-Pff) characterises a gradient from forest clumping (edge) to non-forest clumping (perforated). When Pff = Pf, the model cannot distinguish forest or non-forest clumping. The case of Pf = 1 (interior) represents a completely forested window for which Pff must be 1.

C. Support Vector Machine (SVM): SVM are supervised learning algorithms based on statistical learning theory, which are considered to be heuristic algorithms [21]. SVM map input vectors to a higher dimensional space where a maximal separating hyper plane is constructed. Two parallel hyper planes are constructed on each side of the hyper plane that separates the data. The separating hyper plane maximises the distance between the two parallel hyper planes. An assumption is made that the larger the margin or distance between these parallel hyper planes, the better the generalisation error of the classifier will be. The model produced by support vector classification only depends on a subset of the training data, because the cost function for building the model does not take into account training points that lie beyond the margin [21]. When it is not possible to define the hyper plane by linear equations, the data can be mapped into a higher dimensional space through some nonlinear mapping functions.

A free and open source software – openModeller [22] was used for predicting the probable landslide areas using SVM. openModeller (http://openmodeller.sourceforge.net/) includes facilities for reading landslide occurrence and environmental data, selection of environmental layers on which the model should be based, creating a fundamental niche model and projecting the model into an environmental scenario as shown in Fig. 1.

III. Study Area and Data

The Uttara Kannada district lies 74°9' to 75°10' E longitude and 13°55' to 15°31' N latitude, extending over an area of 10,291 km^2 in the mid-western part of Karnataka state (Fig. 2). It accounts for 5.37 % of the total area of the state with a population above 1.2 million [23]. This region has gentle undulating hills, rising steeply from a narrow coastal strip bordering the Arabian sea to a plateau at an altitude of 500 m with occasional hills rising above 600–860m.

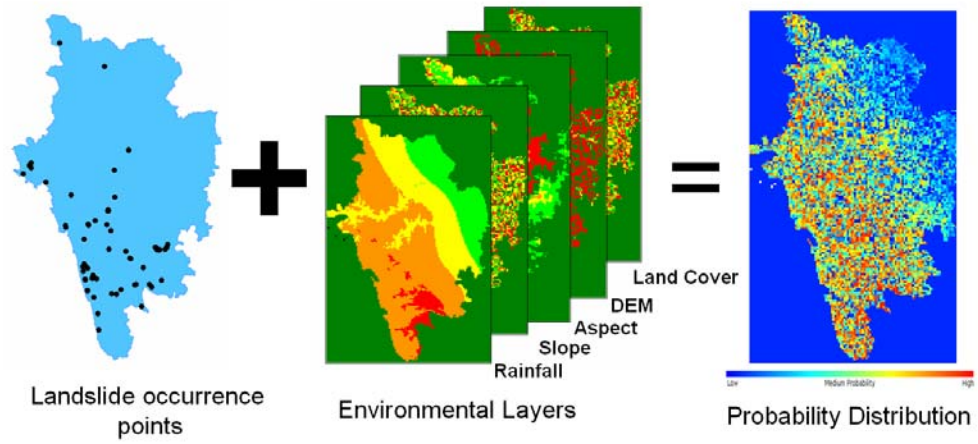

Fig. 1. Methodology used for landslide prediction in openModeller.

Fig. 2. Uttara Kannada district, Karnataka, India.

This district, with 11 taluks, can be broadly categorised into three distinct regions — coastal lands (Karwar, Ankola, Kumta, Honnavar and Bhatkal taluks), mostly forested Sahyadrian interior (Supa, Yellapur, Sirsi and Siddapur taluks) and the eastern margin where the table land begins (Haliyal, Yellapur and Mundgod taluks). Climatic conditions range from arid to humid due to physiographic conditions ranging from plains, mountains to coast.

Survey of India (SOI) toposheets of 1:50000 and 1:250000 scales were used to generate base layers – district and taluk boundaries, water bodies, drainage network, etc. Field data were collected with a handheld GPS. RS data used in the study were Landsat MSS (1973, spatial resolution – 79m), Landsat TM (1989, spatial resolution – 30m), Landsat ETM+ (2000, spatial resolution – 30m) [downloaded from Global Land Cover Facility, http://www.landcover.org] and LISS-III Multi-spectral (2004, spatial resolution – 23.5m) procured from NRSC, Hyderabad, India. Google Earth data (http://earth.google.com) served in pre and post classification process and validation of the results.

Environmental data such as precipitation of wettest month were downloaded from WorldClim – Global Climate Data [http://www.worldclim.org/bioclim]. Other environmental layers (Aspect, DEM, Flow accumulation, Flow direction, Slope, Compound Topographic Index) used for modelling landslide were obtained from USGS Earth Resources Observation and Science (EROS) Center based Hydro1Kdatabase [http://eros.usgs.gov/#/Find_Data/Products_and_Data_Available/gtopo30/hydro/asia]. The global LC change maps were obtained from Global Land Cover Facility, Land Cover Change [http://glcf.umiacs.umd.edu/services/landcoverchange/landcover.shtml; http://www.landcover.org/services/landcoverchange/landcover.shtml]. The spatial resolution of all the data were 1 km. 125 landslide occurrence points of low, medium and high intensity were recorded using handheld GPS from the field and published reports.

IV. Results and Discussion

RS data were geometrically corrected on a pixel by pixel basis and the images were resampled to a common resolution of 30m with a dimension of 7562 x 6790. LC mapping (Fig. 3) was done using normalised difference vegetation index (NDVI) given as

$$\frac{\text{NIR-Red}}{\text{NIR+Red}} \qquad (4)$$

NDVI values range from -1 to +1; increasing values from 0 indicate presence of vegetation (agriculture, forest and plantation) and negative values indicate absence of greenery (builtup, sand, fallow, water) as given in Table I.

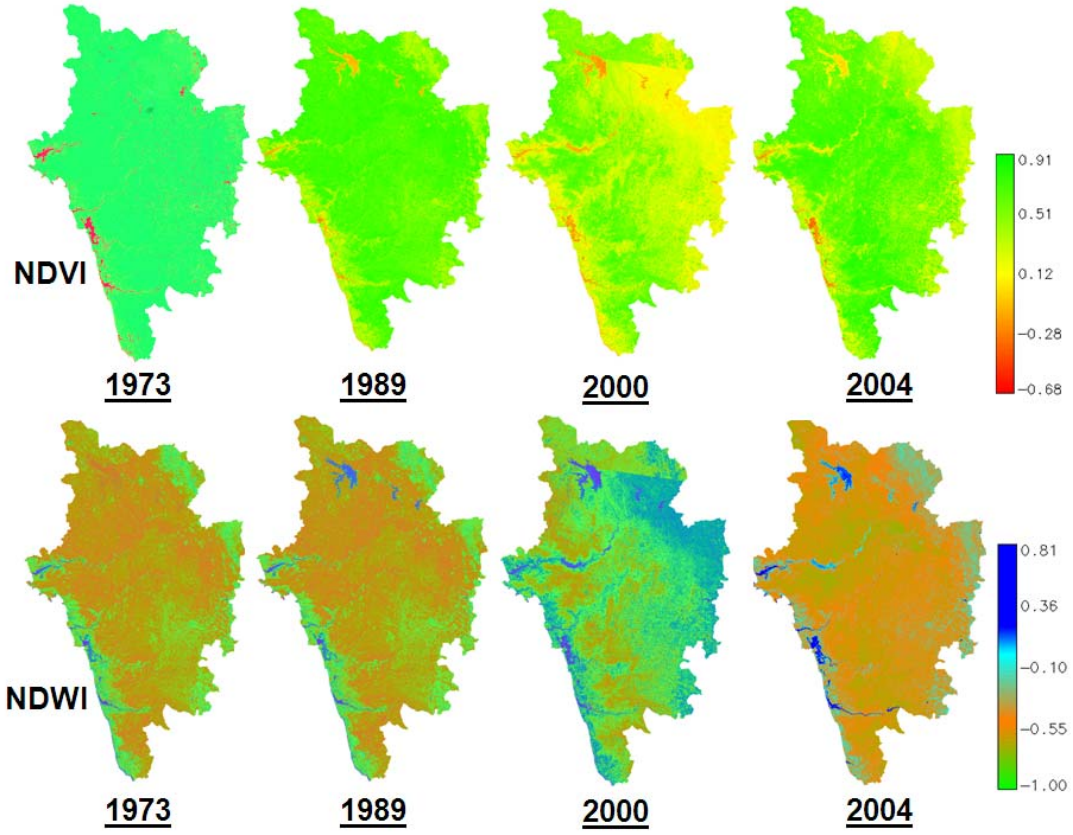

Fig. 3. NDVI and NDWI for Uttara Kannada.

TABLE I: NDVI AND WDVI OF UTTARA KANNADA.

INDEX	NDVI		WDVI	
	VEGETATION (%)	NON-VEGETATION (%)	WATER (%)	NON-WATER (%)
1973	97.82	2.18	1.75	98.25
1989	96.13	3.87	2.20	97.80
2000	94.33	5.67	2.80	97.20
2004	94.00	6.00	2.50	97.50

Mapping of water bodies (Fig. 3) was done using normalised difference water index (NDWI) [24] given as

$$\frac{\text{Green-NIR}}{\text{Green+NIR}} \quad (5)$$

NDWI values above 0 indicate presence of water bodies and values below 0 indicate other classes.

Training pixels were collected from the false colour composite of the respective bands (for time period 1973, 1989, and 2000) since historical data were unavailable. For 2004 data, training data uniformly distributed over the study area collected with pre calibrated GPS were used. The class spectral characteristics for six LU categories (agriculture, builtup / settlement, forest (evergreen, semi-evergreen, deciduous), plantation, waste land / fallow / sand, and water bodies / streams) using RS data were obtained to assess their inter-class separability. and the images were classified using MLC. Temporal classified images (into 6 LC classes – agriculture, built-up, forest, plantation, waste land and water bodies) are shown in Fig. 4 and the statistics are given in Table II. This was validated with the representative field data (covering ~ 10% of the study area) and also using Google Earth image. Producer's, user's, overall accuracy and Kappa values computed are listed in Table III.

Further, five watersheds were delineated from the classified images of four time period as shown in Fig. 5 and the statistics are listed in Table IV. Forest fragmentation model was used to obtain fragmentation indices as shown in Fig. 6 and the statistics are presented in Table V. Forest was categorised into patch, transitional, edge, perforated, and interior types using programs in GRASS GIS (http://wgbis.ces.iisc.ernet.in/foss).

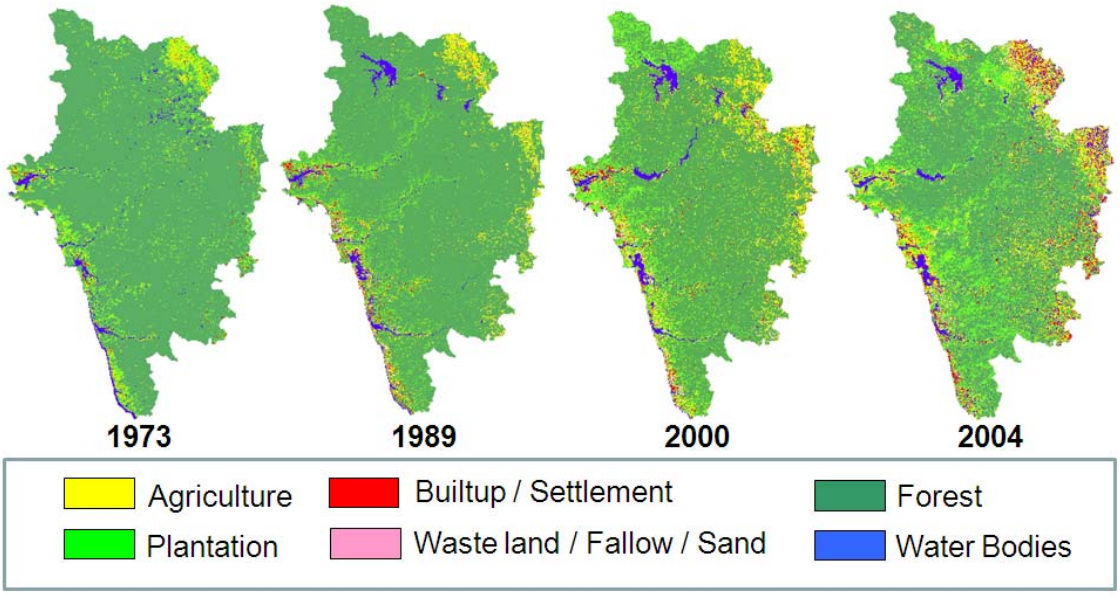

Fig. 4. Temporal classified image of Uttara Kannada district.

TABLE II: LU DETAILS OF UTTARA KANNADA DISTRICT

YEAR	1973		1989		2000		2004	
CLASS	AREA		AREA		AREA		AREA	
	(HA)	(%)	(Ha)	(%)	(Ha)	(%)	(Ha)	(%)
AGRICULTURE	25794	2.51	57465	5.59	97749	9.51	115464	11.23
BUILTUP	4490	0.44	8671	0.84	13674	1.33	27577	2.68
FOREST	897420	87.29	845665	82.25	749877	72.94	627455	61.02
PLANTATION	82439	8.02	85190	8.29	122160	11.88	184340	17.93
WASTE LAND LAND	-	-	8483	0.83	15884	1.54	23456	2.28
WATER BODIES	17995	1.75	22666	2.20	28796	2.80	49924	4.86
TOTAL	1028151	100	1028151	100	1028151	100	1028151	100

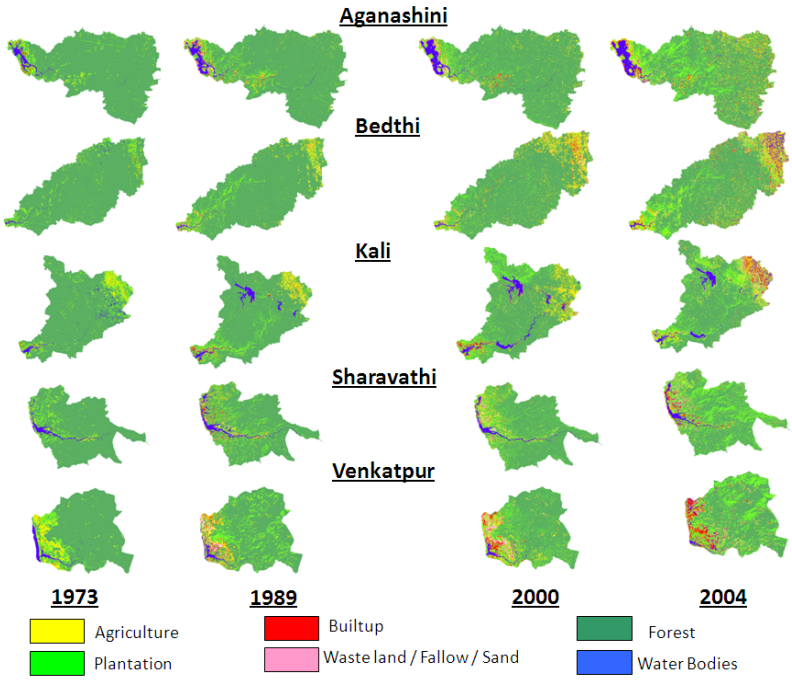

Fig. 5. Temporal LU image of the five rive basins of Uttara Kannada district.

TABLE III: ACCURACY ASSESSMENT OF THE CLASSIFIED IMAGES

YEAR	CATEGORY	USER'S ACCURACY	PRODUCER'S ACCURACY	OVERALL ACCURACY	KAPPA
1973	AGRICULTURE	74.12	77.97	76.89	71.92
	BUILTUP	68.45	65.42		
	FOREST	87.23	85.22		
	PLANTATION	81.27	77.23		
	WASTELAND	85.62	81.21		
	WATER BODIEE	78.50	74.29		
1989	AGRICULTURE	70.43	80.39	75.78	69.82
	BUILTUP	78.78	81.11		
	FOREST	73.96	73.39		
	PLANTATION	79.62	77.19		
	WASTELAND	80.21	77.78		
	WATER BODIEE	31.02	64.82		
2000	AGRICULTURE	81.16	80.47	83.21	79.21
	BUILTUP	84.29	87.50		
	FOREST	87.15	82.54		
	PLANTATION	86.51	87.23		
	WASTELAND	85.22	81.79		
	WATER BODIEE	86.40	97.56		
2004	AGRICULTURE	85.21	84.54	87.83	83.11
	BUILTUP	86.47	83.11		
	FOREST	94.73	96.20		
	PLANTATION	92.27	91.73		
	WASTELAND	88.49	87.88		
	WATER BODIEE	83.13	81.33		

It is to be noted that Supa dam was constructed in late 1970s. Hence this water body is absent in the 1973 Landsat multi-spectral classified image and prominent in the classified images of 1989, 2000 and 2004 (Fig. 4). Also, there was no waste land in 1973 as per the statistics in Table II. All the rivers are perennial since the catchment areas are mainly composed of interior forest. However, eventually there are drastic land cover changes consequent to unplanned developmental activities. In addition, the dams of major rivers in the district have inundated large vegetation areas. These areas have silt deposit at the river beds and have been classified as sand / waste land.

Forest and plantation were considered as a single class - forest and all other classes were considered as non-forest as the extent of LC is a decisive factor in landslides. While the forest fragmentation map produced valuable information, it also helped to visualise the state of forest for tracking the trends and to identify the areas where forest restoration might prove appropriate to reduce the impact of forest fragmentation. Forest fragmentation also depends on the scale of analysis (window size) and various consequences of increasing the window size are reported in [25]. The measurements are also sensitive to pixel size. Nepstad et al., (1999a, 1999b) [26 and 27] reported higher fragmentation when using finer grain maps over a fixed extent (window size) of tropical rain forest. Finer grain maps identify more non-forest area where forest cover is dominant but not exclusive.

The criterion for interior forest is more difficult to satisfy over larger areas. Although knowledge of the feasible parameter space is not critical, there are geometric constraints [28]. For example, it is not possible to obtain a low value of Pff when Pf is large. Percolation theory applies strictly to maps resulting from random processes; hence, the critical values of Pf (0.4 and 0.6) are only approximate and may vary with actual pattern. As a practical matter, when Pf > 0.6, non-forest types generally appeared as "islands" on a forest background, and when Pf < 0.4, forests appeared as "islands" on a non-forest background. Fig. 6 shows the temporal change in forest patch type, revealing that patch, transitional and edge forest are increasing due to deforestation and interior forest is decreasing. The statistics in Table V shows the decrease in forest patch types from 1973 to 2004. Forest fragmentation is a vital indicator that is accountable for environmental changes. With the expansion of human settlement there is higher risk of forest degradation disturbing the biodiversity, affecting the water quality, endangering wildlife survival, habitat protection, etc.

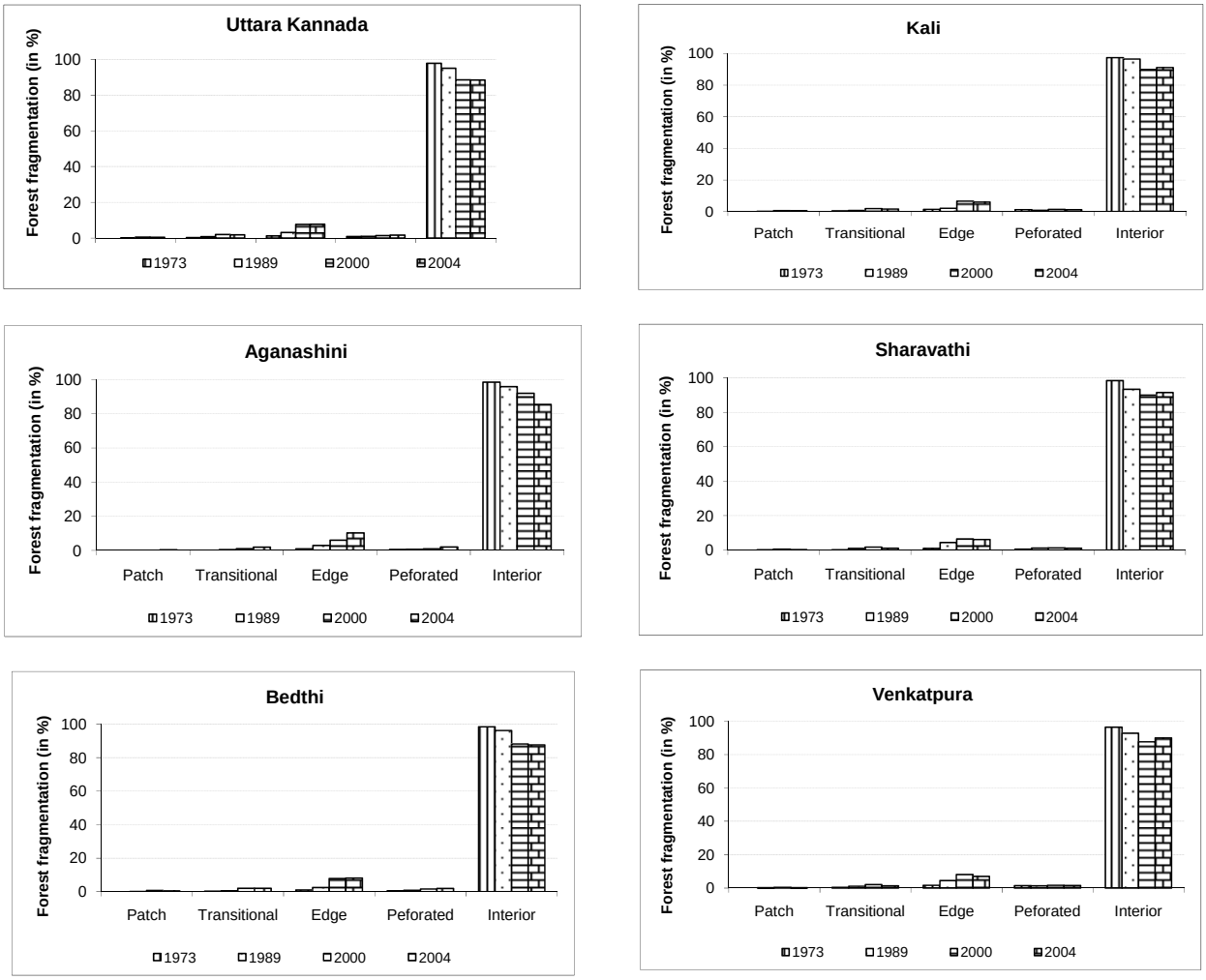

Fig. 6. Temporal Forest fragmentation change of the five river basins of Uttara Kannada district.

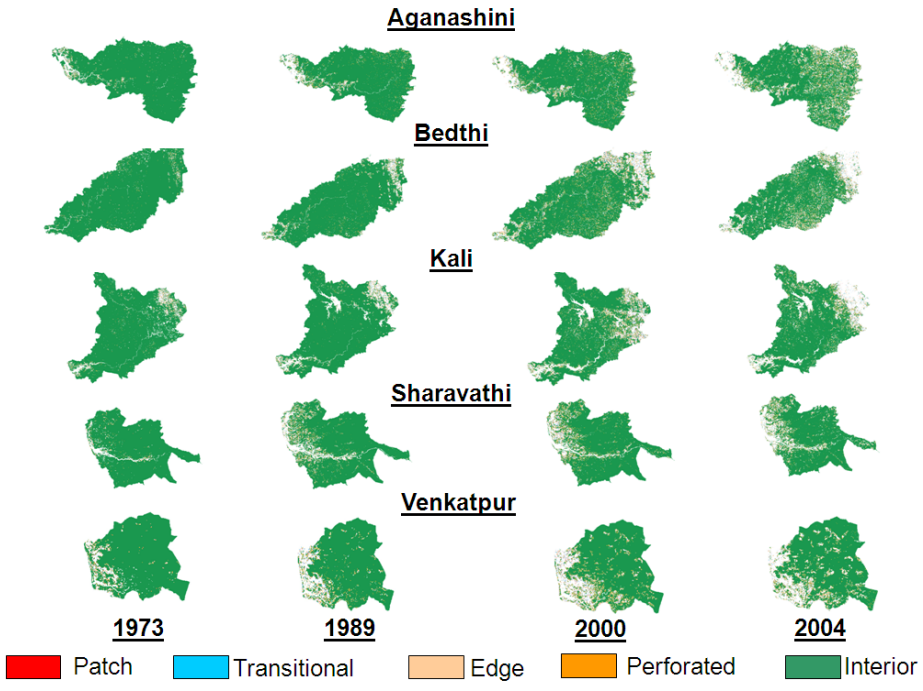

Fig. 6. Forest fragmentation in five river basins in Uttara Kannada district.

TABLE IV: LU DETAILS OF THE FIVE RIVER BASINS (IN HA AND %)

YEAR	CATEGORY	AGANASHINI		BEDTHI		KALI		SHARAVATHI		VENKATPURA	
1973	AGRICULTURE	1886.6	1.4	3616.42	1.3	14294	3.8	1302	1.6	1355.2	5.9
	BUILTUP	627.6	0.5	799.83	0.3	1318.7	0.4	103.976	0.1	74.69	0.3
	FOREST	123500	90	251363	92	320174	86	71536	88	18282	81
	PLANTATION	7930.9	5.8	16315.9	6	31593	8.4	2900	7.3	2289	10
	WASTELAND	-	-	-	-	-	-	-	-	-	-
	WATER BODIES	2662.5	2	1556.7	0.6	6696.8	1.8	2329	2.9	615.9	2.7
1989	AGRICULTURE	4466	3.3	12550.9	4.6	19667	5.3	4110	5.1	1529.7	6.8
	BUILTUP	883.9	0.7	856.9	0.3	2886.6	0.8	784	1.0	404.4	1.8
	FOREST	118724	87	239894	87	303758	81	63686	78	16725	74
	PLANTATION	8217.7	6.0	17783	6.5	34152	9.1	8807	11	3165.8	14
	WASTELAND	784.9	0.6	1360.8	0.5	1696.5	0.5	729	1	508	2.3
	WATER BODIES	3531.6	2.6	1205.8	0.4	11916	3.2	3055	3.8	284	1.3
2000	AGRICULTURE	6179.3	4.5	29413	11	33421	8.9	4781	5.9	1881.3	8.3
	BUILTUP	969.7	0.7	3838.4	1.4	4364	1.2	414.8	0.5	717.6	3.2
	FOREST	11130	81	218541	80	265508	71	59379	73	15363	68
	PLANTATION	12004.6	8.8	16379	6	50542	14	12936	16	3519.7	16
	WASTELAND	1571.8	1.1	3978	1.5	2788.6	0.8	1258	1.6	822.65	3.7
	WATER BODIES	4580.5	3.4	1501.8	0.6	17453	4.7	2404	3	312.9	1.4
2004	AGRICULTURE	13028	9.5	36414	13	36575	9.8	3778.9	4.6	1489.9	6.6
	BUILTUP	2706.5	1.9	5221	1.9	7364.2	1.9	1723.2	2.1	959.98	4.3
	FOREST	84127.8	61	181674	66	232097	62	47020	58	13048	58
	PLANTATION	27836.2	20	35315	13	67093	18	23472	29	5896	26
	WASTELAND	1847.4	1.4	5411	2	10332	2.8	1720.5	2.1	381.97	1.7
	WATER BODIES	7064.4	5.2	9603	3.5	20549	5.5	3484.7	4.3	836.26	3.7

TABLE V: FOREST FRGMENTATION DETAILS OF THE FIVE RIVER BASINS (IN HA)

YEAR	CATEGORY	AGANASHINI	BEDTHI	KALI	SHARAVATHI	VENKATPURA
1973	PATCH	0.59	0.16	1.49	-	0.11
	TRANSITIONAL	189.17	322.04	1050.52	94.99	85.40
	EDGE	1177.55	2398.25	4442.65	729.81	347.26
	PERFORATED	787.33	1478.46	3588.78	457.62	293.29
	INTERIOR	127895.85	261524.81	337778.54	74929.99	19506.20
1989	PATCH	83.69	217.57	333.17	94.67	38.33
	TRANSITIONAL	631.03	1443.65	1995.02	670.22	215.23
	EDGE	3638.08	6198.87	6753.60	3155.90	889.215
	PERFORATED	857.74	1907.86	2526.22	839.13	269.26
	INTERIOR	120188.05	246239.30	322328.53	66064.81	18178.51
2000	PATCH	213.07	1326.61	1637.77	198.690	95.52
	TRANSITIONAL	1201.70	4622.81	5654.96	919.972	390.37
	EDGE	7263.70	18204.16	20319.45	4262.67	1507.74
	PERFORATED	1169.60	3506.29	3977.67	770.327	302.99
	INTERIOR	112006.30	205359.76	280116.92	64838.71	16249.80
2004	PATCH	363.82	947.32	1117.11	144.83	40.424
	TRANSITIONAL	2106.73	4207.65	4414.24	781.60	243.40
	EDGE	11098.47	17250.44	17408.67	4189.86	1274.87
	PERFORATED	2199.95	3942.96	3120.97	717.20	275.79
	INTERIOR	92213.32	186500.95	267026.02	62076.267	16337.97

Precipitations of wettest month along with the seven other layers (as mentioned in section III) were used to predict landslides using SVM as shown in Fig. 7. The landslide occurrence points were overlaid on the probability map to validate the prediction as shown in Fig. 8.

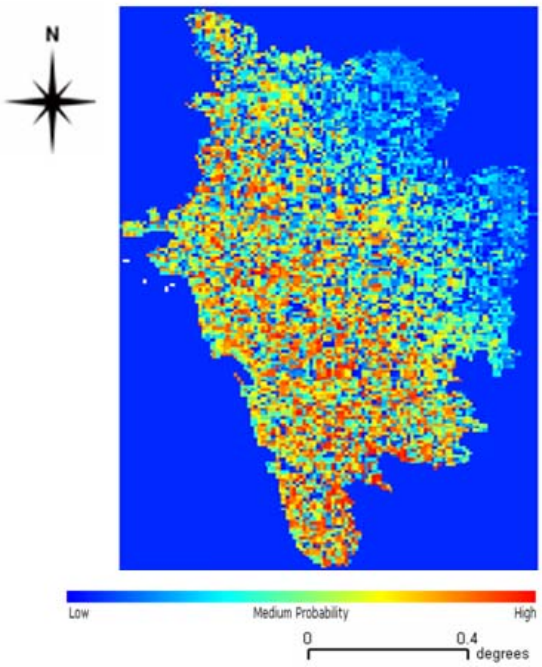

Fig. 7. Probability distribution of the landslide prone areas.

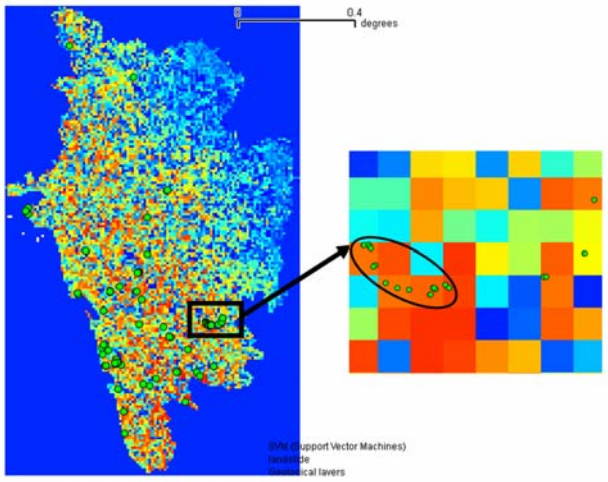

Fig. 8. Validation of the probability distribution of the landslide prone areas by overlaying landslide occurrence points.

The SVM map was 96% accurate with respect to the ground and Kappa values 0.8733 and 0.9083 respectively [29]. Most of the predicted landslide areas as probable landslide prone zones (indicated in red in Fig. 7) reside on terrain that is highly undulating with steep slopes and are frequently exposed to landslides induced by rainfall. Maximum number of landslide points occurring in the undulating terrain, collected from the ground fell in fragmented areas - patch, transitional and edge forest. Fig. 9 shows the landslide occurrence points obtained from ground using handheld GPS overlaid on the classified image of the district (A) and forest fragmentation map (B) based on 2004 RS data. This map indicates that hill slopes with undulating terrain and less vegetation cover (patch, transitional and edge forest) are more susceptible to landslides compared to north-eastern part of the district which has relatively flat terrain with large area utilised under agricultural practices.

The present study makes an effort to quantify forest cover by using fragmentation index for measuring the disturbances due to human impact giving a complete picture of the change that has occurred. The five prominent watersheds of Uttara Kannada district were assessed for quantifying forest fragmentation caused due to anthropogenic disturbances. Forest fragmentation model is useful to visualize state of forest fragmentation for an area and identifying areas where forest restoration might prove appropriate. If the vegetative areas have been cleared, the water retaining capacity of the soil has decreased, triggering landslides in those areas. Hence, there is a immediate need to restore those vegetative by forestation to ensure that the soil is retained on the hill slopes and do not activate any downward movement of the hill tops.

Natural disasters have drastically increased over the last decades. National, state and local government including NGOs are concerned with the loss of human life and damage to property caused by natural disasters. The trend of increasing incidences of landslides occurrence is expected to continue in the next decades due to urbanisation, continued anthropogenic activities, deforestation in the name of development and increased regional precipitation in landslide-prone areas due to changing climatic patterns [30].

V. Conclusion

Landslides occur when masses of rock, earth or debris move down a slope. Mudslides, debris flows or mudflows, are common type of fast-moving landslides that tend to flow in channels. These are caused by disturbances in the natural stability of a slope, which are triggered by high intensity rains. The primary criteria that influence landslides are precipitation intensity, slope, soil type, elevation, vegetation cover and LC type.

In this paper, LU analyses along with forest fragmentation were carried out for five perennial watersheds of Uttara Kannada district. SVM was used to generate probable landslide map. By overlaying the fragmentation map on the landslide probable map, past and future occurrences of landslides can be visualised. It is also evident that degradation of forest and LC change is an important factor that is not only responsible for triggering landslides, but also a major contributor to global warming, climate change, natural resource depletion and consequent detrimental effect on our environment.

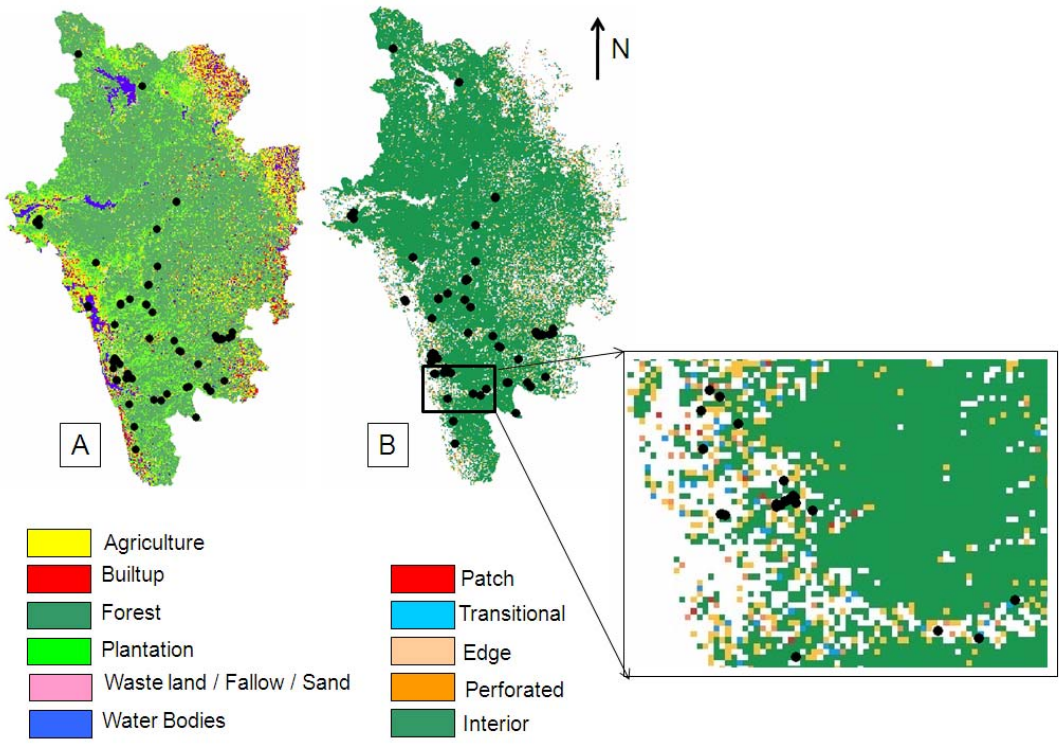

Fig. 9. Landslide susceptibility points overlaid on the classified image of 2004 (A) and forest fragmentation map (B). Black points represent the occurrence of landslide points obtained using handheld GPS.

VI. Acknowledgment

This research was carried out with the financial assistance from Karnataka Biodiversity Board and ISRO -IISc Space Technology Cell (initial work during 2007-2010). The environmental layers were obtained from WorldClim - Global Climate Data. NRSA, Hyderabad provided the LISS IV data used for land cover analysis. We thank USGS Earth Resources Observation and Science (EROS) Center for providing the environmental layers and Global Land Cover Facility (GLCF) for facilitating the Landsat images and Land Cover Change product.

References

[1] G. B. Maithani, "*Non-forestry technology for forest based wasteland development,"* The Indian Forester, vol. 116, pp. 931-937, 1990.

[2] S. N. Rai and A. Saxena, *"The extent of forest fire, grazing and regeneration status in inventoried forest areas in India,"* The Indian Forester, vol. 123, pp. 689-702, 1997.

[3] A. H. Strahler, "*The use of prior probabilities in maximum likelihood classification of remotely sensed data,"* Remote Sensing of Environment, vol. 10, pp. 135-163, 1980.

[4] C. Conese and F. Maselli, "*Use of error matrices to improve area estimates with maximum likelihood classification procedures*," Remote Sensing of Environment, vol. 40, pp. 113-124, 1992.

[5] L. Ediriwickrema and S. Khorram, *"Hierarchical maximum-likelihood classification for improved accuracies,"* IEEE Transactions on Geoscience and Remote Sensing, vol. 35, pp. 810-816, 1997.

[6] M. Zheng, Q. Cai and Z. Wang, "*In: Effect of prior probabilities on maximum likelihood classifier*," Geoscience and Remote Sensing Symposium, 2005, IGARS'05, Proceedings 2005 IEEE International, vol. 6, pp. 3753-3756, 2005.

[7] T. M. Lillesand and R. W. Kiefer, *"Remote Sensing and Image Interpretation,"* Fourth Edition, John Wiley and Sons, 2002, ISBN 9971-51-427-3.

[8] U. Bayarsaikhan, B. Boldgiv, K-R. Kim, K-A. Park and D. Lee, "*Change detection and classification of land cover at Hustai National Park in Mongolia*," International Journal of Applied Earth Observation and Geoinformation, vol. 11, pp. 273-280, 2009.

[9] A. R. John and J. Xiuping, "*Remote Sensing Digital image Analysis: An Introduction*," Springer-Verlag Inc., New York, 1999.

[10] R. O. Duda, P. E. Hart and D, G. Stork, "*Pattern classification*," New York, A Wiley-Interscience Publication, Second Edition, 2000, ISBN 9814-12-602-0.

[11] R. P. Tucker, and J. F. Richards, "*Global deforestation and the nineteenth century world economy*," Duke University Press, Durham, North Carolina, USA, 1983.

[12] B. L. Turner, W. C. Clark, R. W. Kates, J. F. Richards, J. T. Mathews, and W. B. Meyer, "*The Earth as transformed by human action*," Cambridge University Press, Cambridge, UK, 1990.

[13] W. B. Meyer, and B. L. Turner, "*Changes in land use and land cover: a global perspective*," Cambridge University Press, Cambridge, UK, 1994.

[14] R. A. Houghton, "*The worldwide extent of land-use change*," BioScience, vol. 44, pp. 305-313, 1994.

[15] J. D. Hurd, E. H. Wilson, S. G. Lammey, and D. L. Civco, "*Characterization of Forest Fragmentation and Urban Sprawl using time sequential Landsat Imagery*," In ASPRS 2001 Annual Convention, St. Louis, MO, 2001.

[16] R. T. T. Forman, and M. Godron, "*Landscape Ecology*," John Wiley, New York, 1986.

[17] M. G. Turner, "*Landscape ecology: the effect of pattern on process*," Annual Review of Ecology and Systematics, vol. 20, pp. 171-197, 1989.

[18] S. A. Levin, "*The problem of pattern and scale in ecology*," Ecology, vol. 73, pp. 1943-1967, 1992.

[19] T. V. Ramachandra, U. Kumar, P. G. Diwakar and N. V. Joshi, *"Land Cover Assessment using À Trous Wavelet fusion and K-Nearest Neighbour classification,"* In proceedings of the 25th Annual In-House Symposium on Space Science and Technology, ISRO IISc

Space Technology Cell, Indian Institute of Science, Bangalore, India, 29-30 January, 2009.

[20] K., J. Riitters, R. O' Neill. Wickham, B. Jones, and E. Smith, "*Global-scale patterns of forest fragmentation*," Conservation Ecology, vol. 4(2-3), 2000.

[21] T. Kavzoglu , I. Colkesen, "*A kernel functions analysis for support vector machines for land cover classification*," International Journal of Applied Earth Observation and Geoinformation, vol 11, pp. 352-359, 2009.

[22] M. E. S. Munoz, R. Giovanni, M. F. Siqueira, T. Sutton, P. Brewer, R. S. Pereira, D. A. L. Canhos, and V. P. Canhos, *"openModeller- a generic approach to species' potential distribution modeling," Geoinformatica.* DOI: 10.1007/s10707-009-0090-7.

[23] T. V. Ramachandra and A. V. Nagarathna, *"Energetics in paddy cultivation in Uttara Kannada district,"* Energy Conservation and Management, vol. 42(2), pp. 131-155, 2001.

[24] S. K. McFeeters, *"The use of normalized difference water index (NDWI) in the delineation of open water features,"* International Journal of Remote Sensing, vol. 17(7), pp. 1425–1432, 1996.

[25] K. J. Riitters, R. O' Neill. Wickham, B. Jones, and E. Smith, "*Global-scale patterns of forest fragmentation*," Conservation Ecology, vol. 4(2-3), 2000.

[26] D. C. Nepstad, P. Lefebvre, and E. A. Davidson, "*Positive feedbacks in the fire dynamic of closed canopy tropical forests,"* Science, vol. 284, pp. 1832-1835, 1999a.

[27] D. C. Nepstad, A. Verissimo, A. Alencar, C. Nobre, E. Lima, P. Lefebvre, P. Schlesinger, C. Potter, P. Moutinho, E. Mendoza, M. Cochrane, and V. Brooks, "*Large-scale impoverishment of Amazonian forests by logging and fire*," Nature, vol. 98, pp. 505-508, 1999b.

[28] R. V. O'Neill, C. T. Hunsaker, S. P. Timmins, B. L. Jackson, K. B. Jones, K. H. Ritters, and J. D. Wickham, "*Scale problems in reporting landscape pattern at the regional scale*," Landscape Ecology, vol. 11, pp. 169-180, 1996.

[29] T. V. Ramachandra, U. Kumar, Bharath H. Aithal, P. G. Diwakar and N. V. Joshi, "*Landslide Susceptible Locations in Western Ghats: Prediction through open Modeller,"* In proceedings of the 26th Annual In-House Symposium on Space Science and Technology, ISRO-IISc Space Technology Cell, Indian Institute of Science, Bangalore, India, 28-29 January, 2010.

[30] T. V. Ramachandra, M. D. Subashchandran and Anant Hegde Ashisar, *"Landslides at Karwar, October 2009: Causes and Remedial Measures,"* ENVIS Technical Report: 32, Environmental Information System, Centre for Ecological Sciences, Bangalore, 2009.